performed by Desert Analytics, Tuscon, AZ. All infrared solution spectra were obtained on a Mattson Cygnus 25 FTIR spectrometer using 0.1- or 0.5-mm potassium bromide cells. NMR spectra were obtained on a JEOL FX90Q (^{1}H) or a Bruker WM360 (^{1}H, ^{13}C) spectrometer and are reported as positive downfield from TMS. Chromatographic separations were performed by using untreated silica gel (60-200 mesh).

EI mass spectra were recorded on a VG TRIO 1 instrument using the VG LAB BASE data system operating with a 70-eV electron beam and a 150-μA trap current. All other spectra including the **2a** decomposition studies were recorded on a VG ZAB-HF in the fast atom bombardment (FAB) ionization mode. The FAB ion source used was the standard VG Analytical, Inc., system equipped with a saddle field atom gun. Xenon was used for the bombarding fast atom beam; typical operating conditions were beam energies of 8 keV and neutral beam currents equivalent to 1.5 mA supplied by an ION TECH (Model B 50) current and voltage regulator/meter.

Materials. **1a**,[7b,c] **1b**,[16] **3a**,[17] and **3b**[17] were prepared by published procedures. Me_3NO was purchased from Eastman Kodak Co. as the dihydrate and dried by removing the water as an azeotrope with benzene.

Synthesis of KS_2CH.[18] To a solution of $KB(O^iPr)_3H$[19] (50 mmol) in THF (30 mL) was added CS_2 (4.0 g, 53 mmol) via syringe. The solution turned from clear to orange initially, and yellow-orange solids eventually precipitated from the solution. The solution was stirred for 1 h, after which it was concentrated and the solids were filtered from the solution. Recrystallization of the solids from ethanol produced 2.4 g (41% yield) of yellow crystals of KS_2CH. KS_2CD was prepared similarly by using $KB(O^iPr)_3D$.

Synthesis of 2a. **1a** (0.5 g, 1.8 mmol) and CS_2 (1 mL) in CH_2Cl_2 (30 mL) were stirred at room temperature for 30 min, during which the solution turned from yellow to red. The solution was then filtered, the solvent was removed by vacuum, and the product was recrystallized from acetone/hexane, producing 0.48 g (75% yield) of rust red crystals. ^{1}H NMR ($(CD_3)_2CO$): δ 2.25 (s, 18 H, CH_3), 11.44 (s, 1 H, SC(S)H). ^{13}C{^{1}H} NMR ($(CD_3)_2CO$, 210 K): δ 224.1 (s, CO), 108.2 (s, C_6Me_6), 16.5 (s, CH_3). IR (THF): ν(CO) 1969, 1921 cm^{-1}; ν(CS) 1245, 1011, and 647 cm^{-1}. See Table I for mass spectral data. Anal. Calcd for $C_{15}H_{19}O_2S_2Mn$: C, 51.42; H, 5.47. Found: C, 50.95; H, 5.23.

Alternate Method. To a mixture of **3a** (0.5 g, 1.12 mmol) and Me_3NO (0.13 g, 1.73 mmol) was added THF (50 mL) with stirring for 30 min at 0 °C, turning the solution from yellow to purple. To this was added a 10-mL THF solution of KSC(S)H (0.17 g, 1.46 mmol). The resultant solution was stirred for an additional 30 min at room temperature, followed by filtration and elution from a column of silica with acetone/hexane. Recrystallization from acetone/hexane produced 0.28 g (70% yield) of rust red crystals. $(\eta^6$-$C_6Me_6)Mn(CO)_2SC(S)D$ was prepared in a similar manner by using KSC(S)D.

Synthesis of 2b. To **3b** (0.362 g, 1.0 mmol) and Me_3NO (0.075 g, 1.0 mmol) was added 50 mL of THF at 0 °C, resulting in a purple solution. After 30 min of stirring, a 10-mL THF solution of KSC(S)H (0.116 g, 1.0 mmol) was added, followed by an additional 1 h of stirring at 0 °C. Upon concentration of the solvent followed by addition of hexane and cooling to -20 °C, 0.16 g (60% yield) of red crystals were obtained after filtration. ^{1}H NMR ($(CD_3)_2CO$): δ 6.19 (s, 6 H, C_6H_6), 11.68 (s, 1 H, SC(S)H). IR (THF): ν(CO) 1995, 1948 cm^{-1}; ν(CS) 1240, 992, and 625 cm^{-1}. Mass spectral data (FAB MS): parent ion at m/z 267, $(M + H)^+$. Instability of the product precluded elemental analysis.

Reaction of 2a and 4a. A solution of **4a** was prepared by the addition of Me_3NO (0.075 g, 1.0 mmol) to **3a** (0.446 g, 1.0 mmol) in 20 mL of THF at 0 °C followed by 30 min of stirring. To this purple solution was then added a 20-mL solution of **2a** (0.350 g, 1.0 mmol), followed by an additional 30 min of stirring at room temperature. The resulting red solution was evaporated to dryness under reduced pressure to give a red solid, which was redissolved in a minimal amount of CH_2Cl_2 and recrystallized with the addition of hexane and cooling to -20 °C, producing 0.65 g (85% yield) of **5**-PF_6. ^{1}H NMR ($(CD_3)_2CO$): δ 2.17 (s, 36 H, CH_3), 10.75 (s, 1 H, μ-SC(S)H). IR (THF): μ(CO) 1975, 1928 cm^{-1}. The mass spectral data are presented in Table I.

Reaction of 5-PF_6 and KS_2CH. To a CH_2Cl_2 (20 mL) solution of **5**-PF_6 (0.011 g, 0.014 mmol) was added an equal molar amount KS_2CH at room temperature. A gradual loss in the concentration of **5**-PF_6 and the formation of **2a** was observed spectroscopically (IR and ^{1}H NMR spectroscopy) over time, and the reaction was complete after 6 h of stirring at room temperature.

Reaction of 5-PF_6 and CH_3Li. To a stirred solution of **5**-PF_6 (0.012 g, 0.016 mmol) in THF (20 mL) was added an equal molar amount of CH_3Li via syringe. There was an immediate color change from red to orange, and IR data indicated the formation of **2a**, $(\eta^6$-$C_6Me_6)Mn(CO)_2CH_3$ (**8**), and $((\eta^6$-$C_6Me_6)Mn(CO)_2)_2$ (**9**).

(16) Rush, P. K.; Noh, S. K.; Brookhart, M. *Organometallics* **1986**, *5*, 1745.
(17) Preparation of (arene)manganese carbonyl cations: (a) Winkhaus, G.; Pratt, L.; Wilkinson, G. *J. Chem. Soc.* **1961**, 3807. (b) Pauson, P. L.; Segal, J. A. *J. Chem. Soc., Dalton Trans.* **1975**, 1677. (c) Winkhaus, G.; Singer, H. *Z. Naturforsch., B: Anorg. Chem., Org. Chem.* **1963**, *18B*, 418.
(18) Other methods of preparation: (a) Binder, H.; Diamantikos, W. *Z. Naturforsch., B: Anorg. Chem., Org. Chem.* **1983**, *38B*, 203. (b) Engler, V. R.; Gattow, G.; Dräger, M. *Z. Anorg. Allg. Chem.* **1972**, *390*, 64.
(19) Brown, H. C.; Nazer, B.; Sikorski, J. A. *Organometallics* **1983**, *2*, 634.

Contribution from the Department of Chemistry, Faculty of Science, Hiroshima University, Higashi-senda-machi, Naka-ku, Hiroshima 730, Japan

A Hydrogen-Bonding Mode in the Ion Association of the *d*-Tartrate Anion with the Λ-*ob*$_3$-Tris((1*R*,2*R*)-diaminocyclohexane)cobalt(III) Cation

Tsutomu Mizuta, Kazuo Toshitani, and Katsuhiko Miyoshi*

Received May 25, 1990

Introduction

It is well-known that oxo anions such as PO_4^{3-}, SO_4^{2-}, and SeO_3^{2-} form intimate ion pairs in solution with tris(diamine)metal complex cations with a *lel*$_3$ conformation.[1-3] This is because a set of three N-H groups on the triangular face of the *lel*$_3$ complex are disposed almost parallel to the C_3 axis so as to form triple linear hydrogen bonds to a set of three oxygen atoms of the oxo anions along the C_3 axis. Actually, such association modes have been found in the crystal structures of *lel*$_3$-$[Co(en)_3]_2[HPO_4]_3 \cdot 9H_2O$[4] and *lel*$_3$-$[Co(en)_3][AsO_4] \cdot 3H_2O$[5] (en = 1,2-diaminoethane). In contrast, these oxo anions show a much weaker affinity for the *ob*$_3$ complexes[1,6-10] with a set of three N-H groups oblique to the C_3 axis, because the hydrogen bonds formed are inevitably bent and are thus weak.

In the course of our X-ray crystallographic study on ion-association modes of the *d*-(*R*,*R*)-tartrate dianion (abbreviated as the *d*-tart ion hereafter) with the *lel*$_3$-tris(diamine)cobalt(III) complex cations,[11-13] a common face-to-face contact mode has been found. In this contact mode, the three oxygen atoms, two alcoholic and one carboxylic, of the *d*-tart ion are nicely disposed among the three parallel N-H groups on the triangular face of the *lel*$_3$ complex to form three bifurcated hydrogen bonds to

(1) *lel*$_3$ refers to a conformation in which each C-C bond in the three five-membered chelates lies parallel to the C_3 axis, while *ob*$_3$ refers to the one in which it lies oblique to this axis.
(2) Mason, S. F.; Norman, B. J. *Proc. Chem. Soc., London* **1964**, 339. Mason, S. F.; Norman, B. J. *J. Chem. Soc. A* **1966**, 307.
(3) Smith, H. L.; Douglas, B. E. *Inorg. Chem.* **1966**, *5*, 784.
(4) Duesler, E. N.; Raymond, K. N. *Inorg. Chem.* **1971**, *10*, 1486.
(5) Rius, J.; Gali, S. *Cryst. Struct. Commun.* **1982**, *11*, 829.
(6) Ogino, K. *Bull. Chem. Soc. Jpn.* **1969**, *42*, 447.
(7) Harnung, S. E.; Kallesoe, S.; Sargeson, A. M.; Schaffer, C. E. *Acta Chem. Scand., A* **1974**, *28*, 385. Bond, A. M.; Hambley, T. W.; Mann, D. R.; Snow, M. R. *Inorg. Chem.* **1987**, *26*, 2257.
(8) Yoshikawa, Y.; Yamasaki, K. *Coord. Chem Rev.* **1975**, *28*, 205. Sakakibara, K.; Yoshikawa, Y.; Yamatera, H. *Bull. Chem. Soc. Jpn.* **1979**, *52*, 2725.
(9) Harnung, S. E.; Sorensen, B. S.; Creaser, I.; Maegaard, H.; Pfenninger, U.; Schaffer, C. E. *Inorg. Chem.* **1976**, *15*, 2123.
(10) Kojima, M.; Fujita, J. *Bull. Chem. Soc. Jpn.* **1981**, *54*, 2691.
(11) Kushi, Y.; Kuramoto, M.; Yoneda, H. *Chem. Lett.* **1976**, 135.
(12) Mizuta, T.; Tada, T.; Kushi, Y.; Yoneda, H. *Inorg. Chem.* **1988**, *27*, 3836.
(13) Mizuta, T.; Toshitani, K.; Miyoshi, K.; Yoneda, H. *Inorg. Chem.* **1990**, *29*, 3020.

0020-1669/91/1330-0572$02.50/0

Table I. Crystallographic Data for Λ-*ob*$_3$-[Co(*R*,*R*-chxn)$_3$]Cl(*d*-tart)·3.5H$_2$O

cryst formula	$C_{18}H_{42}N_6Co$ $C_4H_4O_6Cl\cdot3.5H_2O$	fw	648.1
		space group	$P2_122_1$
a, Å	10.711 (3)	*T*, °C	20
b, Å	12.832 (4)	ρ_{calcd}, g cm^{-3}	1.35
c, Å	23.181 (6)	ρ_{obsd}, g cm^{-3}	1.34
V, Å^3	3186 (2)	μ(Mo Kα), cm^{-1}	5.88
Z	4	λ(Mo Kα), Å	0.71069
R^a	0.049	$R_w{}^b$	0.047

$^a R = \sum(||F_o| - |F_c||)/\sum|F_o|$. $^b R_w = [\sum w(|F_o| - |F_c|)^2/\sum w(F_o)^2]^{1/2}$.

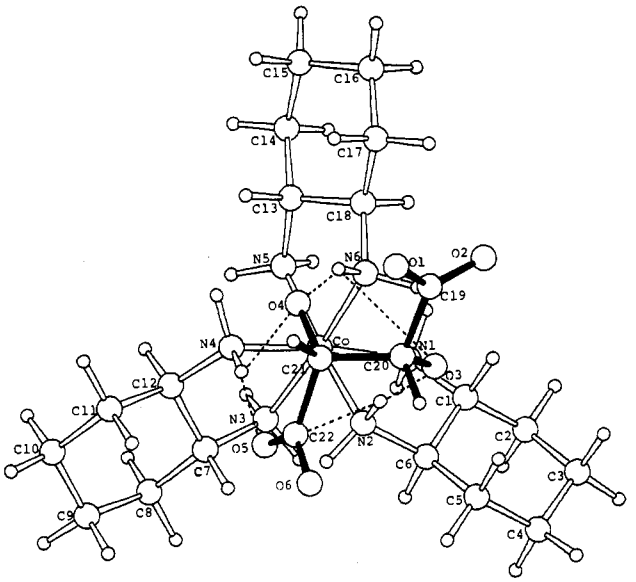

Figure 1. Drawing of the face-to-face contact mode viewed along the C_3 axis with the numbering schemes for Λ-*ob*$_3$-[Co(*R*,*R*-chxn)$_3$]Cl(*d*-tart)·3.5H$_2$O. The relevant hydrogen bonds are shown by dotted lines.

them.[13,14] As a result, these hydrogen bonds are all moderately bent and are thus weaker than the linear ones formed in the contact modes of some oxo anions with the *lel*$_3$ complexes. That is, the *d*-tart ion prefers to form as many hydrogen bonds as possible to the *lel*$_3$ complex, unlike the usual oxo anions, which favor triple linear hydrogen bonds to it.

It is notable here that *d*-tart ion also shows a weaker affinity for the *ob*$_3$ complexes in solution,[6,13] indicating that its interaction with the *ob*$_3$ complex must be in total weaker than the three bifurcated hydrogen bonds to the *lel*$_3$ complex. In the present study, the crystal structure analysis has been carried out on the title complex salt with *d*-tart and Cl ions, to explore how the *d*-tart ion interacts with the *ob*$_3$ complex.

Experimental Section

Λ-*ob*$_3$-[Co(*R*,*R*-chxn)$_3$]Cl(*d*-tart)·3.5H$_2$O (*R*,*R*-chxn = (1*R*,2*R*)-diaminocyclohexane), formed by mixing Λ-*ob*$_3$-[Co(*R*,*R*-chxn)$_3$]Cl$_3$[9] with sodium *d*-tartrate in water, was dissolved in water, and orange crystals were grown on evaporation. A crystal of suitable size was selected and was mounted on a Syntex R3 diffractometer. Details of data collection and refinement of the structure are summarized in Table I. In the refinement, one water molecule was found to lie on the symmetry element. The absolute configuration of the complex was confirmed to be Λ by the anomalous dispersion technique.[15] The final refinement including calculated hydrogen atom coordinates with isotropic temperature factors converged the *R* and R_w values to 0.049 and 0.047, respectively. The weighting scheme used was $w = (\sigma_{cs}{}^2)^{-1}$, where σ_{cs} is the standard deviation obtained from the counting statistics. All the computations were carried out on a HITAC M-680 H computer and the programs used were UNICS-III[16] and ORTEP.[17] All atomic coordinates except for hydrogen atoms are given in Table II.

Table II. Atomic Coordinates in Λ-*ob*$_3$-[Co(*R*,*R*-chxn)$_3$]Cl(*d*-tart)·3.5H$_2$O with Esd's in Parentheses

atom	*x*	*y*	*z*	*B*, Å^2
Co	0.21527 (6)	0.73624 (5)	0.16818 (3)	1.8
N1	0.0871 (4)	0.6644 (3)	0.1214 (2)	2.3
N2	0.2944 (4)	0.5994 (3)	0.1715 (2)	2.3
N3	0.1210 (4)	0.7124 (3)	0.2405 (2)	2.5
N4	0.3426 (4)	0.7964 (3)	0.2196 (2)	2.1
N5	0.1376 (4)	0.8739 (3)	0.1566 (2)	2.3
N6	0.3144 (3)	0.7704 (3)	0.0995 (2)	2.0
C1	0.1370 (5)	0.5634 (4)	0.1000 (2)	2.2
C2	0.0376 (6)	0.4878 (5)	0.0801 (2)	3.5
C3	0.1014 (7)	0.3843 (5)	0.0636 (3)	5.1
C4	0.1797 (7)	0.3400 (4)	0.1120 (3)	4.6
C5	0.2769 (6)	0.4175 (4)	0.1328 (2)	3.3
C6	0.2104 (5)	0.5180 (4)	0.1498 (2)	2.3
C7	0.2076 (5)	0.7173 (4)	0.2897 (2)	2.5
C8	0.1421 (6)	0.7244 (5)	0.3478 (2)	3.3
C9	0.2415 (6)	0.7355 (5)	0.3949 (2)	4.7
C10	0.3265 (7)	0.8286 (5)	0.3839 (2)	4.5
C11	0.3891 (5)	0.8213 (5)	0.3247 (2)	3.5
C12	0.2901 (5)	0.8104 (4)	0.2788 (2)	2.3
C13	0.2184 (6)	0.9358 (4)	0.1170 (2)	2.6
C14	0.1519 (6)	1.0302 (4)	0.0904 (2)	3.7
C15	0.2409 (7)	1.0829 (4)	0.0475 (3)	4.5
C16	0.2879 (7)	1.0083 (4)	0.0019 (3)	4.7
C17	0.3504 (6)	0.9135 (4)	0.0291 (2)	3.4
C18	0.2604 (5)	0.8617 (4)	0.0708 (2)	2.2
C19	0.7044 (5)	0.6458 (4)	0.0477 (2)	2.7
C20	0.6396 (5)	0.5969 (4)	0.1009 (2)	2.3
C21	0.6503 (5)	0.6641 (4)	0.1542 (2)	2.1
C22	0.6125 (4)	0.6004 (4)	0.2079 (2)	1.9
O1	0.8101 (4)	0.6832 (4)	0.0561 (2)	4.7
O2	0.6466 (4)	0.6402 (3)	0.0015 (2)	3.6
O3	0.5123 (3)	0.5744 (3)	0.0899 (1)	2.9
O4	0.5811 (3)	0.7576 (3)	0.1464 (1)	2.7
O5	0.5183 (3)	0.6280 (3)	0.2361 (1)	2.7
O6	0.6778 (3)	0.5226 (3)	0.2183 (1)	3.1
Cl	−0.0354 (2)	0.9511 (1)	0.2735 (1)	5.1
OW1	−0.0712 (3)	0.5533 (3)	0.2135 (2)	3.5
OW2	0.0000 (0)	0.7596 (5)	0.0000 (0)	5.0
OW3	−0.1184 (4)	0.8570 (4)	0.1184 (2)	5.9
OW4	−0.2974 (5)	0.9085 (4)	0.2084 (3)	9.0

Table III. Selected Hydrogen-Bond Distances and Angles[a]

O··H–N	O··H, Å	O··N, Å	O··H–N, deg
O3··H–N2	2.03 (2.17)	3.02 (3.07)	167.8 (149.2)
O3··H–N6	3.00 (2.50)	3.29 (3.21)	98.0 (128.3)
O4··H–N6	2.11 (2.05)	3.05 (2.98)	157.2 (152.8)
O4··H–N4	2.47 (2.34)	3.10 (3.01)	119.9 (127.4)
O5··H–N4	1.92 (2.06)	2.88 (3.05)	161.8 (156.8)
O5··H–N2	2.52 (2.47)	2.84 (3.17)	93.2 (127.0)

[a] The values for the *lel*$_3$ contact mode[11] are given in parentheses.

Results and Discussion

Figure 1 shows the molecular structures and numbering schemes of the complex cation and the *d*-tart ion in the crystal, where the complex takes a Λ-*ob*$_3$ configuration and the *d*-tart ion takes a normal conformation compared to those reported so far. The bond distances and angles within these ions are in good agreement with those reported earlier,[13,18] and they are given in the supplementary material (Table ST3).

It is seen in Figure 1 that the *d*-tart ion lies on the triangular face of the complex with the four O atoms (O2, O3, O4, and O5) directed to it, making a face-to-face contact with the complex, and that three of these O atoms, two alcoholic and one carboxylic, are involved in the multiple hydrogen bonds to the three oblique N–H protons on the face; each O atom is placed between two of

(14) Bernal, I.; Korp, J. D.; Creaser, I. I. *Aust. J. Chem.* **1984**, *37*, 2365.
(15) On the basis of all the non-hydrogen atoms, the *R* value converged to 0.066 for a Λ-configuration and to 0.074 for a Δ-configuration.
(16) Ashida, T. In *The Universal Crystallographic Computation Program System*; Sakurai, T., Ed.; The Crystallographic Society of Japan: Tokyo, 1979.
(17) Johnson, C. K. Report ORNL-3794; Oak Ridge National Laboratory: Oak Ridge, TN, 1976.
(18) Kobayashi, A.; Marumo, F.; Saito, Y. *Acta Crystallogr., Sect. B* **1972**, *28*, 2709. Kobayashi, A.; Marumo, F.; Saito, Y. *Acta Crystallogr., Sect. C* **1983**, *39*, 807.

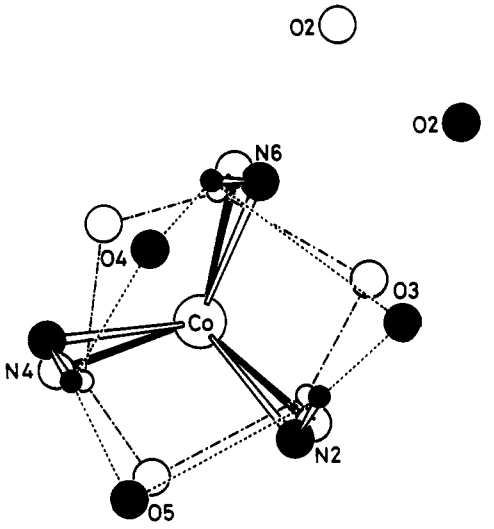

Figure 2. Projection of the four oxygen atoms to the triangular face of the complex cation for Λ-ob_3-[Co(*R*,*R*-chxn)$_3$]Cl(*d*-tart)·3.5H_2O (filled circles) and Λ-lel_3-[Co(en)$_3$]Br(*d*-tart)·5H_2O (open circles). The relevant hydrogen bonds are shown by dotted lines.

the three N–H groups and is hydrogen bonded to them simultaneously.[19] A numerical comparison of the hydrogen bonds pertinent to the contact mode is made in Table III.

Now, the above contact mode with the ob_3 complex is examined in detail and is called here the ob_3 contact mode. For comparison, the contact mode found in the crystal of Λ-lel_3-[Co(en)$_3$]Br(*d*-tart)·5H_2O[11] is quoted as the typical lel_3 contact mode, and the hydrogen bonds formed in it are also compared in Table III. To compare the two modes visually, the positions of the four O atoms directed to the complex are projected to the triangular face in Figure 2, such that the three N–H protons of the ob_3 complex may be best superimposed on those of the lel_3 complex.

It is evident in Figure 2 that the two contact modes are surprisingly similar in that the three O atoms are each placed between two of the three N–H groups and are each connected with them through one long and one short hydrogen bond;[14] it is probably due to an intrinsic property of the *d*-tart ion that its three O atoms are apt to lie among these N–H protons but not just on them.[20] However, the two modes are significantly different with respect to the hydrogen-bond angles (Table III). That is, in the ob_3 contract mode, the three short hydrogen bonds (O3··H–N2, O4··H–N6, and O5··H–N4) are fairly linear and are thus very strong, while the remaining three long ones (O3··H–N6, O4··H–N4, and O5··H–N2) are significantly bent and are thus weak. In the lel_3 contact mode, on the other hand, the three short and three long hydrogen bonds are all moderately bent, though the longer ones tend to be more bent[21] as in the ob_3 contact mode. These differences are to be expected, because when the conformation is changed from lel_3 to ob_3, with the three O atoms left almost intact, each N–H proton comes to be in a position to form a shorter and more linear hydrogen bond to one O atom and a longer and more bent hydrogen bond to the other O atom. As a result, of the six moderately bent hydrogen bonds formed in the lel_3 mode, the three short ones are strengthened but the three long ones are weakened upon the conformational change to ob_3. In this way, since the ob_3 contact mode found here is quite reasonable, this mode is likely to be adopted in solution as well.

Some pieces of experimental evidence are available which indicate that the *d*-tart ion shows a weaker affinity for the ob_3 complex in solution,[6,13] like the usual oxo anions do. Then, if the *d*-tart ion adopts in solution the contact modes similar to those shown in Figure 2, the overall hydrogen-bonding interaction in the ob_3 mode must be surpassed by that in the lel_3 mode. However, since the three short and three long hydrogen bonds formed in the lel_3 mode are further strengthened and weakened, respectively, upon the conformational change to ob_3, the overall interaction is not so drastically diminished in the ob_3 mode. In contrast, the usual oxo anions suffer a serious damage to their hydrogen-bonding interaction with the complex upon the conformational change; the three originally linear and strong hydrogen bonds are all forced to be bent and are weakened appreciably.[22] Therefore, it is expected that the usual oxo anions serve as a more effective selector than *d*-tart ion in the chromatographic separation of these conformational isomers.[23] Our preliminary study has estimated the conventional separation factor[13] to be 2.38 for Na_2SO_4 (0.1 M) and 1.88 for Na_2*d*-tart (0.1 M) in the chromatographic separation of Λ-lel_3- and Λ-ob_3-[Co(chxn)$_3$]$^{3+}$ on an SP-Sephadex ion-exchange column. These experimental results are consistent with our assertion that the usual oxo anions are more readily subjected to the effect of the chelate conformation, when they form ion pairs with these metal–amine complex cations through the hydrogen-bonding interaction.[8,10,23] In contrast, the *d*-tart ion is rather insensitive to the conformational change; it manages to form intimate hydrogen bonds to both lel_3 and ob_3 complexes.

Supplementary Material Available: Full listings of the crystallographic data (Table ST1), positional and isotropic thermal parameters for hydrogen atoms (Table ST2), bond distances and angles (Table ST3), and anisotropic thermal parameters for non-hydrogen atoms (Table ST4) (7 pages); a listing of observed and calculated structure factor amplitudes (Table ST5) (17 pages). Ordering information is given on any current masthead page.

(19) The second hydrogen bond (O3··H–N6) in the ob_3 contact mode given in Table III might be too long to be regarded as an actual bond.
(20) Yoneda, H. *J. Chromatogr.* **1984**, *313*, 59.
(21) Taylor, R.; Kennard, O. *Acc. Chem. Res.* **1984**, *17*, 320.
(22) For example: Vedani, A.; Dunitz, J. D. *J. Am. Chem. Soc.* **1985**, *107*, 7653.
(23) Searle, G. H. *Aust. J. Chem.* **1977**, *30*, 2625.

Contribution from the Department of Chemistry, Oregon State University, Gilbert Hall 153, Corvallis, Oregon 97331-4003

The Cubane Structure of $Mo_4O_4(\mu_3\text{-}O)_4(OSi(CH_3)_3)_4(HN(CH_3)_2)_4$[†]

Gyu Shik Kim, Douglas A. Keszler,* and Carroll W. DeKock*

Received April 3, 1990

Introduction

Compounds of transition-metal clusters, that is compounds containing metal–metal bonds, have been actively studied over the last two decades.[1] Among these molecules, the cubane structure containing the core $M_4(\mu_3\text{-}X)_4$ has been an important and recurrent structural motif in a number of molecular systems, having now been observed with the metals M = V, Cr, Mo, W, Re, Fe, Os, Co, and Pt bound by a variety of ligands. Also, the oxo Mo cubane $Mo_4(\mu_3\text{-}O)_4$ has recently been observed in condensed oxide phases, forming in layered structures[2] and three-dimensional microporous solids.[3] In all these systems, the cubane may be highly distorted, with the nature of the distortions arising from the number of electrons available for bonding and the characteristics of the ligands.[4,5]

Our recent interests have involved the preparation of new oxo Mo compounds by the cocondensation of MoO_3 and various silicon reagents; these syntheses have afforded a variety of new dioxo–alkoxo (siloxo)–Mo compounds.[6] Here we wish to describe the structure and synthesis of the new compound $Mo_4O_4(\mu_3\text{-}O)_4(OSi(CH_3)_3)_4(HN(CH_3)_2)_4$, which was crystallized as a minor

[†] This work was presented at the 43rd Northwest Regional Meeting of the American Chemical Society, Spokane, Washington, June 29–July 1, 1988; INORG 128.

0020-1669/91/1330-0574$02.50/0